Molecular Cancer Therapeutics

Optimizing Therapeutic Effect of Aurora B Inhibition in Acute Myeloid Leukemia with AZD2811 Nanoparticles

Nicolas Floc'h[1], Susan Ashton[2], Paula Taylor[2], Dawn Trueman[2], Emily Harris[2], Rajesh Odedra[2], Kim Maratea[3], Nicola Derbyshire[2], Jacqueline Caddy[2], Vivien N. Jacobs[2], Maureen Hattersley[4], Shenghua Wen[4], Nicola J. Curtis[2], James E. Pilling[5], Elizabeth J. Pease[5], and Simon T. Barry[1]

Abstract

Barasertib (AZD1152), a highly potent and selective aurora kinase B inhibitor, gave promising clinical activity in elderly acute myeloid leukemia (AML) patients. However, clinical utility was limited by the requirement for a 7-day infusion. Here we assessed the potential of a nanoparticle formulation of the selective Aurora kinase B inhibitor AZD2811 (formerly known as AZD1152-hQPA) in preclinical models of AML. When administered to HL-60 tumor xenografts at a single dose between 25 and 98.7 mg/kg, AZD2811 nanoparticle treatment delivered profound inhibition of tumor growth, exceeding the activity of AZD1152. The improved antitumor activity was associated with increased phospho-histone H3 inhibition, polyploidy, and tumor cell apoptosis. Moreover, AZD2811 nanoparticles increased antitumor activity when combined with cytosine arabinoside. By modifying dose of AZD2811 nanoparticle, therapeutic benefit in a range of preclinical models was further optimized. At high-dose, antitumor activity was seen in a range of models including the MOLM-13 disseminated model. At these higher doses, a transient reduction in bone marrow cellularity was observed demonstrating the potential for the formulation to target residual disease in the bone marrow, a key consideration when treating AML. Collectively, these data establish that AZD2811 nanoparticles have activity in preclinical models of AML. Targeting Aurora B kinase with AZD2811 nanoparticles is a novel approach to deliver a cell-cycle inhibitor in AML, and have potential to improve on the clinical activity seen with cell-cycle agents in this disease. *Mol Cancer Ther; 16(6); 1031–40. ©2017 AACR.*

Introduction

Acute myeloid leukemia (AML) is the most prevalent leukemia diagnosed in adults. AML is a cancer of the blood and bone marrow derived from the "common myeloid progenitor," which gives rise to myeloblasts, red blood cells, and megakaryocytes. It is characterized by disease infiltration in the bone marrow and blood of abnormally/poorly differentiated myeloblasts, red blood cells, or platelets. AML progresses rapidly and aggressively and requires immediate treatment. The majority of cases occur in patients aged over 60 years of age, and the median age of diagnosis is 67 (1). Despite recent progress in understanding the genetic basis of AML (2), treatment options have changed little in the last 30 years (3–5). Treatment is divided in two phases (6, 7). The first phase of treatment or "Induction" targets leukemic cells in blood and reduces the number of blasts in the bone marrow. Currently, patients often receive intravenous anthracycline given for 3 days combined with a 7-day continuous infusion of cytosine arabinoside (Ara-C). Finally, a maintenance therapy usually consists of intermediate doses of Ara-C.

The treatment for AML is therefore very aggressive. Unfortunately, older AML patients are often unfit to receive such intensive therapy. In the United States, less than 40% of AML patients receive chemotherapy for their disease (8). There are few alternative treatment options. The most common is low-dose Ara-C (LDAC), while recently azacitidine has been introduced. These approaches modestly improve the median overall survival by 5 and 8.5 months, respectively (9–11). Another therapeutic option, such as decitabine, has also been investigated (12). The cure rate for AML varies from 35%–40% in adult patients who are 60 years of age or younger and decreases to 5%–15% for patients over 60 years of age (6). Given the elevated morbidity for AML patients, the development of new therapeutic options that improve durability of the response is critical.

Given the aggressive hyperproliferative nature of AML, it is thought that improvements in outcome could be delivered by agents targeting cell cycle. Barasertib (AZD1152), a prodrug rapidly converted to AZD2811 (formerly known as AZD1152-hQPA), has been developed as a highly potent and selective Aurora kinase B inhibitor (13–16). Inhibition of Aurora kinase

[1]IMED Oncology, AstraZeneca, Cambridge, United Kingdom. [2]IMED Oncology, AstraZeneca, Macclesfield, United Kingdom. [3]IMED Drug Safety & Metabolism, AstraZeneca, Gatehouse Park, Waltham, Boston, Massachusetts. [4]IMED Oncology, AstraZeneca, Gatehouse Park, Waltham, Boston, Massachusetts. [5]IMED Discovery Sciences, AstraZeneca, Cambridge, United Kingdom.

Note: Supplementary data for this article are available at Molecular Cancer Therapeutics Online (http://mct.aacrjournals.org/).

Corresponding Author: Simon T. Barry, AstraZeneca, Robinson Way, Cambridge CB2 0RE, United Kingdom. Phone: +44 7789744771; E-mail: simon.t.barry@astrazeneca.com

doi: 10.1158/1535-7163.MCT-16-0580

B induced chromosome misalignments during mitosis and failed cytokinesis leading to polyploidy and eventually to cell death (17). Barasertib has shown promising benefits in phase II clinical trials in AML patients with a 35% improvement in the objective complete response rate (18). Despite this clinical proof of concept, the mode of administration as a 7-day infusion has led to a discontinuation of the development of barasertib. To address this challenge, we have developed a nanoparticle encapsulating a small molecule Aurora B kinase inhibitor, AZD2811 (19, 20).

Here we show activity of this novel nanoparticle formulation in preclinical models of AML. AZD2811 nanoparticle has the potential to induce a more durable response relative to AZD1152 in preclinical models of AML.

Methods

TGI and pharmacodynamic studies in tumor xenograft models

All animal studies were conducted in accordance with U.K. Home Office legislation, the Animal Scientific Procedures Act 1986, as well as the AstraZeneca Global Bioethics policy. All experimental work is outlined in project licence 40/3483, which has gone through the AstraZeneca Ethical Review Process. Studies in the United States were conducted in accordance with the guidelines established by the internal Institutional Animal Care and Use Committee (IACUC) and reported following the ARRIVE (Animal Research: Reporting *In Vivo* Experiments) guidelines (21). Randomization of animals onto study was based on initial tumor volumes to ensure equal distribution across groups. A power analysis was performed whereby group sizes were calculated to enable statistically robust detection of tumor growth inhibition (TGI, >6 per group) or pharmacodynamic endpoint (>4 per group).

All animals included on studies were greater than 5–6 weeks old at the time of cell implant. Human AML HL-60 cells (Origin: ATCC, CCL-240) were cultured in RPMI1640 supplemented with 20% (v/v) FCS and 1% (v/v) glutamine and cultured in a humidified incubator with 7.5% CO_2 at 37°C. HL-60 xenografts were established by subcutaneous implantation of 1×10^7 cells per animal, in 100 μL of cell suspension including 50% Matrigel, into the dorsal left flank of female CB17 SCID mice. Human AML OCI-AML3 cells (Origin: DSMZ, ACC 582) were cultured in Alpha-MEM with 20% (v/v) FCS and 1% (v/v) glutamine and cultured in a humidified incubator with 5% CO_2 at 37°C. OCI-AML3 xenografts were established by subcutaneous implantation of 5×10^6 cells per animal, in 100 μL of cell suspension including 50% Matrigel, into the dorsal right flank of female CB 17 SCID mice. Human AML MV4-11 cells (Origin: ATCC, CRL-9591) were cultured in Iscove's modified Dulbecco's medium (IMDM) supplemented with 10% (v/v) FCS in a humidified incubator with 5% CO_2 at 37°C. MV4-11 xenografts were established by subcutaneous implantation of 1×10^7 cells per animal, in 100 μL of cell suspension, into the dorsal right flank of female CB17 SCID mice. Human AML MOLM-13 cells (Oncotest) were cultured in RPMI supplemented with 10% (v/v) FCS + gentamycin in a humidified incubator with 5% CO_2 at 37°C. MOLM-13 xenografts were established by tail vein injection of 5×10^6 cells into the tail vein of female NOG mice. Cytogenetics of the different cell lines used is reported in Supplementary Table S1.

In the subcutaneous xenograft model, tumors were measured two to three times weekly by caliper and volume calculated using elliptical formula ($\pi/6 \times$ width $\times$ width $\times$ length). Tumor growth inhibition (%TGI) from the start of treatment was assessed by comparison of the geometric mean change in tumor volume for the control and treated groups. Tumor regression was calculated as the percentage reduction in tumor volume from baseline value: % Regression = (1 − RTV) × 100%, where RTV is the geometric mean relative tumor volume. Statistical significance was evaluated using a one-tailed *t* test.

In the MOLM-13, disseminated xenograft model tumor load was determined in peripheral blood and in the bone marrow by FACS analysis. Briefly peripheral blood and bone marrow cells were resuspended in 10 mL 1× ACK-lysis buffer (0.15 mol/L NH_4CL, 10 mmol/L $KHCO_3$, and 0.1 mmol/L EDTA) and lysed for 1–3 minutes at room temperature. Cells were then centrifuged at 300 × *g* for 10 minutes at 4°C, washed once with 10 mL 2% FCS buffer, and resuspended in backflow. Cells were then transferred to a 96-well plate (5×10^5 cells/well if sufficient, if not possible, they were divided equally among the wells) and pelleted by centrifugation of the plates at 400 × *g* for 3 minutes at 4°C and the supernatant was removed. Fc-block antibody (10 μL/well) was added to each well and plates were incubated for 15 minutes at room temperature. Then specific antibodies [CD45: BD Biosciences (catalog no. 564105) and HLA-ABC BD (catalog no. 561346)] were added and plates were incubated at 4°C protected from light for 30 minutes. Following another washing step (centrifugation of the plates at 400 × *g* for 3 minutes at 4°C), cells were resuspended in 250 μL FACS buffer and analyzed using an Attune Focusing Cytometer [blue (488 nm)/violet (405 nm) laser configuration].

All *in vivo* studies were dosed either intravenously with placebo nanoparticles, AZD1152, or AZD2811 nanoparticle or intraperitoneally with Ara-C. The nanoparticles and Ara-C were diluted to required concentration in 0.9% physiologic saline. AZD1152 was diluted to required concentration in 0.3 mol/L Tris buffer, pH 9.

Tumor pharmacodynamic studies

For acute pharmacodynamic studies, SCID mice bearing HL-60 xenografts were dosed intravenously with a single bolus dose of placebo nanoparticles, AZD2811 nanoparticle, or AZD1152. Tumors were excised postmortem at specified time points and fixed in 10% buffered formalin for 24 to 48 hours, and then processed to paraffin block.

Sections (4 μm) were deparaffinized with xylene and rehydrated through graded alcohols into water. Antigen retrieval was carried out in a Milestone RHS microwave rapid histoprocessor for 5 minutes at 110°C in pH 6 citrate buffer (Dako S1699). Tissues were placed on a Lab Vision Autostainer, endogenous peroxidase was blocked with 3% H_2O_2 for 10 minutes, followed by washing twice in TBS/0.05% Tween (TBS-T). For phosphohistone H3 (pHH3), serum-free protein block (Dako; X0909) was applied for 15 minutes prior to incubation with primary antibody (Upstate Biotechnology 06-570; 1/1,000 dilution) for 1 hour. For cleaved caspase-3, samples were incubated with avidin and biotin (Vector SP-2001) for 20 minutes each, prior to a goat serum block (diluted according to kit Vector VK-6101) for 20 minutes followed by addition of primary antibody (Abcam ab32042; 1:400 dilution) for 1 hour. For detection of pHH3, sections were incubated for 30 minutes with Rabbit EnVision polymer detection system (Dako; K4003). For detection of cleaved caspase-3, samples were incubated with the secondary antibody and Vector Elite ABC reagent according to the manufacturer's instructions (Vector PK-6101 Rabbit Kit). All

samples were developed in liquid 3,3-diaminobenzidine (DAB; Dako K3468) for 10 minutes. Sections were then counterstained with Carazzi hematoxylin, dehydrated, cleared, and mounted with coverslips. All washes were performed in TBS-T and all steps were conducted at room temperature.

Cleaved caspase-3 and pHH3 immunoreactivity were scored semiquantitatively by a pathologist as follows: 0 = <5% positive cells; 1 = 5%–10% positive cells; 2 = 11%–25% positive cells; 3 = 26%–50%; 4 = >50% positive cells. Hematoxylin and eosin (H&E)-stained sections were scored for karyomegaly, an indicator of polyploidy, using the same system.

Bone marrow pharmacodynamic studies

Han Wistar rats were dosed intravenously with placebo nanoparticles or AZD2811 nanoparticles. Femurs were excised postmortem at specified time points and fixed in 10% buffered formalin for 24 to 48 hours, decalcified in an EDTA solution and processed to paraffin block. Femurs were scored semiquantitatively by a pathologist for a reduction in bone marrow cellularity using a scoring system, where 0 = no change, 1 = minimal, 2 = mild, 3 = moderate, and 4 = severe change. Bone marrow from the contralateral femur was flushed using 50% FCS/50% PBS and analyzed by flow cytometry. Nucleated bone marrow cells were analyzed using a method adapted from Saad and colleagues (22). The bone marrow cell suspensions were filtered through a 100-μm disposable filter device (Filcons, Dako) then underlayered with 1-mL FBS (Sigma) and centrifuged at 300 × *g* for 5 minutes at 4°C. The cell pellet was resuspended in 4 mL of ice-cold PBS containing 0.5% BSA. FITC-conjugated mouse anti-rat CD45 (5 μL) and 10 μL of phycoerythrin (PE)-conjugated mouse anti-rat CD71 mAbs (Serotec) were added to 100 μL of adjusted bone marrow cell suspension, mixed well, and incubated on ice in the dark for 20 minutes. Cells were washed with ice cold PBS containing 0.5% BSA and recentrifuged. The resulting cell pellet was resuspended in 0.4 mL ice-cold PBS containing 0.5% BSA then 20 μL of LDS-751 staining solution (Molecular Probes) was added and kept in the dark for 20 minutes, prior to flow cytometric analyses. Sample analysis was performed using FACSDiva.

Complete blood counts

Di-potassium EDTA anticoagulated peripheral whole blood samples were analyzed on an Advia 2120i automated hematology analyzer with veterinary software (Siemens). Total white blood cell counts and neutrophil count were calculated for each group.

AML lines *in vitro* culture condition and assays

Cell lines were purchased from ATCC or obtained from academic laboratories from 2006 to 2014. All cell lines were authenticated at AstraZeneca cell banking using DNA fingerprinting short tandem repeat (STR) assays and confirmed to be free of bacterial and viral contaminations by IDEXX. All cell lines were used within 15 passages, and less than 6 months.

MV4-11, HL-60, MOLM-13, and KG1-a cell lines were cultured and assayed in RPMI1640 phenol red–free supplemented with 10% (v/v) FCS + 2 mmol/L glutamine. All cell lines were maintained and assayed under humidified conditions of 37°C and 5% CO_2.

Cells were seeded in 96-well plates at a density allowing for logarithmic growth during the 6-day assay. Cells were exposed to an AZD2811 monotherapy dose response (eight-point dose response 10–0.001 μmol/L). Following 6-day compound incubation, cell viability was assessed through the addition of Alamar Blue reagent. The reaction was stopped with 0.5% SDS solution and fluorescence read on a Tecan Saffire II. The dose at which 50% inhibition of viability (IC_{50}) was achieved was then established for each cell line. For assessment of nuclear area, cells were stained with Hoescht (1:1,000) in RPMI1640, pipetting the cells up and down three times to disperse any clumps. After 20 minutes, the plates were centrifuged at 300 × *g* for 5 minutes. Five images per well at 20× magnification were taken for assessment of nuclear area.

Results

AZD2811 nanoparticle causes profound and sustained tumor regression in the AML subcutaneous HL-60 xenograft model

Inhibiting Aurora B kinase reduces proliferation and induces polyploidy across an *in vitro* panel of human AML cancer cell lines (Supplementary Fig. S1; Supplementary Table S2; refs. 14, 23). Monotherapy activity was observed *in vivo* when AZD2811 nanoparticle was administered to animals bearing the AML HL-60 xenograft model (Fig. 1). AZD2811 nanoparticle dosed at 25 mg/kg induced 21% tumor regression (day 19) when compared with the placebo nanoparticle group (Fig. 1A; Table 1). When given either as a single dose of 50 or 25 mg/kg on day 1 and day 3, AZD2811 nanoparticle induces very similar tumor regression (87% and 93% respectively, at day 19) relative to the placebo nanoparticle group (Fig. 1A; Table 1). This demonstrates that the same total amount of AZD2811 nanoparticle given as a single dose or as two separate doses gives similar efficacy.

To establish whether increasing dose gives greater benefit, the dose response was explored in more detail. A single dose of 98.7 mg/kg (maximum deliverable dose) AZD2811 nanoparticle gave 93% tumor regression (day 19; Fig. 1A; Table 1), but achieved a more durable tumor regression. Indeed, for half of the tumors, regression was achieved for at least 70 days (conclusion of study; Fig. 1C). Interestingly, a similar total drug dosage of AZD1152, the phosphate prodrug of the active drug AZD2811 (25 mg/kg for four consecutive days) showed only modest efficacy establishing that AZD2811 nanoparticle has potential to improve on AZD1152 (Supplementary Fig. S2). At the different doses explored, AZD2811 nanoparticle was well tolerated, and minimal body weight loss was observed compared with predose starting body weight (Fig. 1B).

AZD2811 nanoparticle decreases the level of pHH3, induces polyploidy, and apoptosis in the AML subcutaneous HL-60 xenograft model

A number of different biomarkers can be used to assess the impact of AZD2811 nanoparticle within the tissues (15). Pharmacodynamic effects were confirmed by assessing pHH3 inhibition coupled to an increase in polyploidy. To explore the relationship between efficacy and target modulation, mice bearing HL-60 xenografts were treated with either placebo nanoparticle, AZD2811 nanoparticle, or AZD1152. Following administration of AZD2811 nanoparticle, the level of pHH3 was reduced at both 48 and 96 hours. This decrease was dose dependent (Fig. 2A). Consistent with the decrease of pHH3, an increase in polyploidy (Fig. 2B) and an increase in apoptosis (Fig. 2C) as measured by the level of cleaved caspase-3 was observed. The induction of apoptosis peaked at 48 hours following treatment and was greatest in

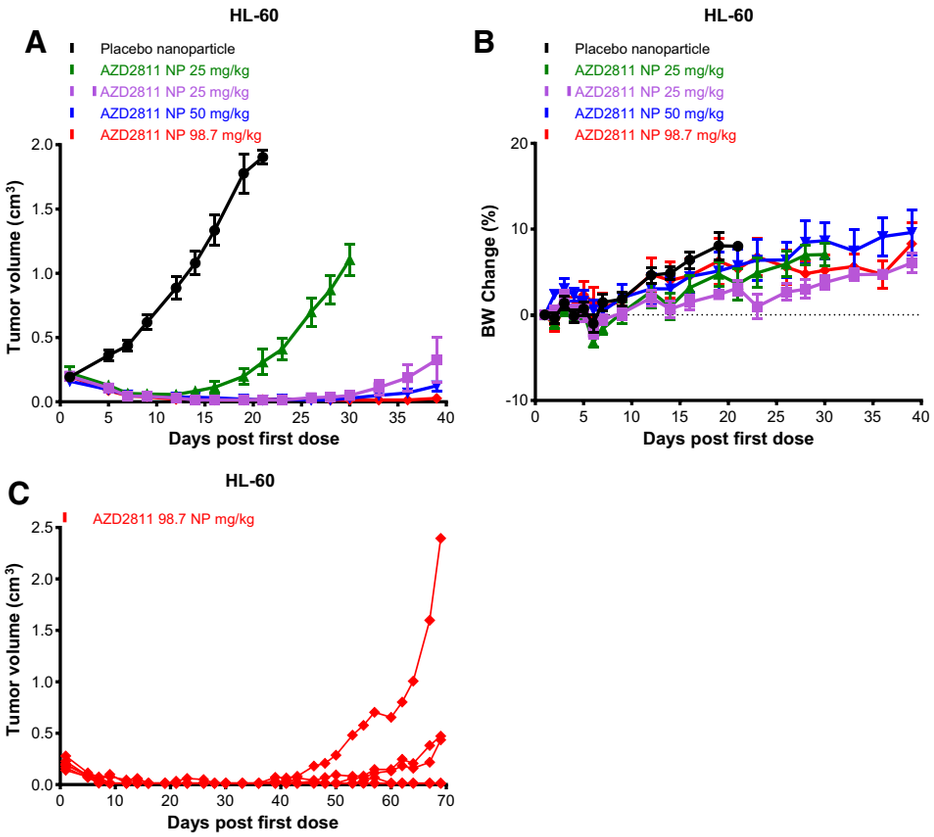

Figure 1.
AZD2811 nanoparticle induces dose-dependent TGI in the HL-60 AML xenograft model *in vivo*. **A,** Dose-related TGI after one cycle of the AZD2811 nanoparticle in the subcutaneous HL-60 xenograft model in CB17 SCID mice. Data are represented as mean ± SEM ($n = 10$ for placebo nanoparticle and $n = 6$ for AZD2811 nanoparticle-treated groups). **B,** Minimal body weight loss is observed at these efficacious doses. Data expressed as percentage change in CB17 SCID mouse body weight relative to start body weight on day 0. **C,** Tumor growth inhibition for individual mice ($n = 6$) after a single dose of AZD2811 nanoparticle 98.7 mg/kg on day 1 in CB17 SCID mice. Placebo nanoparticle, black circle; AZD2811 NP 25 mg/kg, green triangle (tip up); AZD2811 NP 25 mg/kg D1/D3, pink square; AZD2811 NP 50 mg/kg, green triangle (tip down); AZD2811 NP 98.7 mg/kg, red diamond.

the group dosed with 98.7 mg/kg. The data suggest an initial wave of apoptosis occurs which is reduced to a lower rate at 96 hours. However, the level of polyploidy is sustained at 96 hours with both doses is consistent with the inhibition of tumor growth for at least 10 days following treatment. These data are consistent with achieving sustained Aurora B kinase inhibition. In contrast, administration of AZD1152 did not reduce the level of pHH3 at the timepoints explored, nor did it induce polyploidy or apoptosis (Fig. 2).

AZD2811 nanoparticle combined with Ara-C provides durability of response in the AML subcutaneous HL-60 xenograft model

Having established monotherapy activity of AZD2811 nanoparticle, we next explored the benefit of combining AZD2811 nanoparticle with Ara-C in the HL-60 xenograft model (Fig. 3). Combining AZD2811 nanoparticle (25 mg/kg) with Ara-C (12.5 mg/kg) increased regression and the durability of response when compared with Ara-C alone or AZD2811 nanoparticle alone (Fig. 3A). The combination of AZD2811 nanoparticle and Ara-C showed 74% regression at the end of study when compared with AZD2811 nanoparticle monotherapy (Fig. 3A). In contrast, AZD1152 used at a higher total dose compared with AZD2811 nanoparticle (25 mg/kg for four consecutive days) only provides a modest duration of response in combination with Ara-C (Supplementary Fig. S3). AZD2811 nanoparticle alone or in combination with Ara-C was well tolerated, minimal body weight loss was observed compared with predose start body weight (Fig. 3C). Taken together, this data suggest that one way to achieve the durability of response could be combining AZD2811 nanoparticle with Ara-C.

Impact of high dose of AZD2811 nanoparticle on bone marrow

In AML, achieving drug exposure in the bone marrow during the induction phase is essential. Previously, we established that AZD2811 nanoparticle used at 25 mg/kg on day 1 and day 3 has minimal effect on bone marrow compared with AZD1152, and did not impact the white blood cell or neutrophil count (19). Having established that AZD2811 nanoparticle improves treatment efficacy in the HL-60 xenograft model, we then analyzed the impact of a higher dose of AZD2811 nanoparticle on the bone marrow of the Han Wistar rat, which better reflects the effects of treatment on human bone marrow (ref. 24; Fig. 4A).

Table 1. Percentage TGI or regression in the HL-60 xenograft model following AZD2811 nanoparticle treatment compared with placebo nanoparticle dosed controls at day 19 post-first dose

Dose of AZD2811 NP	Day of dosing	%TGI	%Regression	*P* (one-tailed student *t* test)
25 mg/kg	D1	>100	21	<0.001 day 19
25 mg/kg	D1/D3	>100	93	<0.001 day 19
50 mg/kg	D1	>100	87	<0.001 day 19
98.7 mg/kg	D1	>100	93	<0.001 day 19

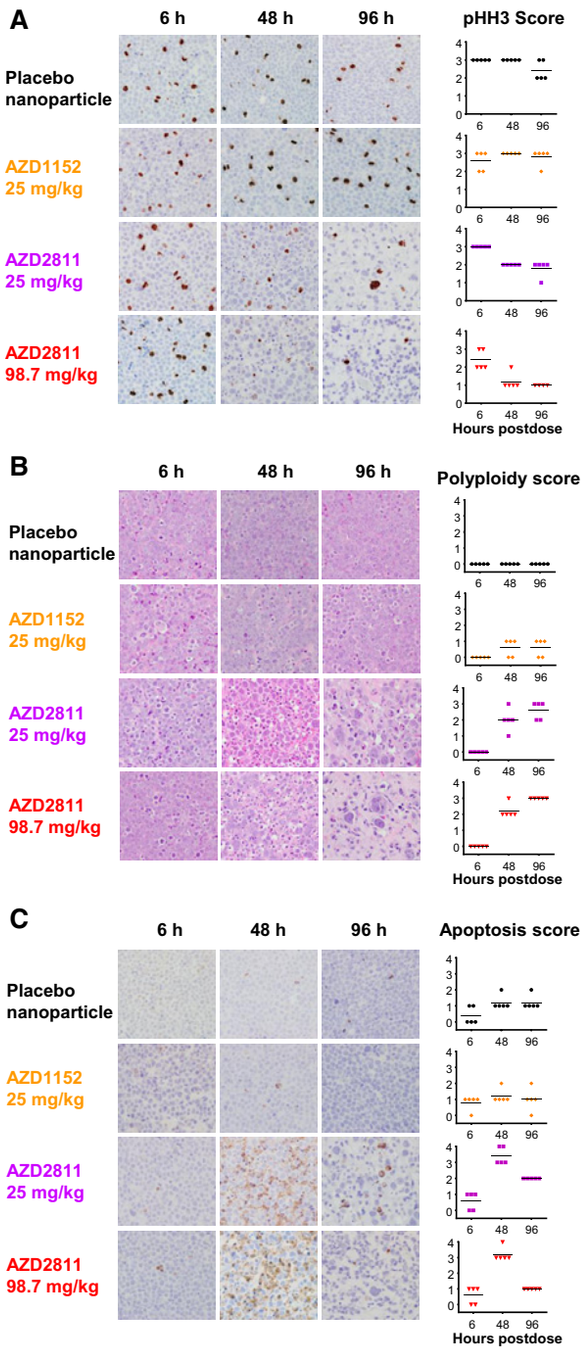

Figure 2.
The AZD2811 nanoparticle given as monotherapy reduces the level of pHH3, a marker of mitosis, induces polyploidy, and induces apoptosis in the HL-60 AML xenograft model growth *in vivo*. **A,** pHH3 IHC staining and scatter dot plots of semiquantitative pHH3 score, from tumors collected at 6, 48, and 96 hours following the first dose of AZD2811 nanoparticle or AZD1152. **B,** H&E staining and scatter dot plots of semiquantitative polyploidy scores from tumors collected at 6, 48, and 96 hours following the first dose of AZD2811 nanoparticle or AZD1152. **C,** Cleaved caspase-3 IHC staining and semiquantitative cleaved caspase-3 score from tumors collected at 6, 48, and 96 hours following the first dose of AZD2811 nanoparticle or AZD1152. All images were captured at 40× magnification.

Han Wistar rats were dosed with AZD2811 nanoparticle at 25 mg/kg on day 1 and day 3. As previously observed, this dose and schedule was well tolerated. Indeed, no bone marrow toxicity was detected by semiquantitative pathology assessment (Fig. 4B and C; Supplementary Fig. S4A) or FACS analysis quantifying the percentage of total nucleated cell (TNC) in the bone marrow (Fig. 4D and E). However, a single dose of AZD2811 nanoparticle at 50 or 98.7 mg/kg resulted in a decrease in bone marrow cellularity (Fig. 4C). Microscopically, decreased cellularity was accompanied by dilated marrow sinuses on days 5 and 9 (Supplementary Fig. S4A). This finding was confirmed by FACS analysis quantifying the percentage of TNC. AZD2811 nanoparticle dosed at 50 and 98.7 mg/kg respectively, induced a 24% and 62% decrease in the percentage of TNCs at day 5.

At these doses, no obvious toxicity was seen on the small intestine, another organ commonly impacted by these agents. Collectively these data support the conclusion that a high dose of AZD2811 nanoparticle gives sufficient bone marrow exposure, whereas a lower dose can be used with minimal impact on the bone marrow.

The effects on the bone marrow were mirrored in the peripheral blood. Following reduction of bone marrow cellularity, there is a rapid effect on neutrophil levels in peripheral blood, indeed change in neutrophils can be used as a surrogate measure of impact on bone marrow. Following AZD2811 nanoparticle treatment, a cardiac blood puncture was performed at the time of each bone marrow analysis (Fig. 4A). As observed in the bone marrow, AZD2811 nanoparticle given at 25 mg/kg on day 1 and day 3 did not impact the peripheral white blood cell (WBC) or the neutrophil count (Fig. 4F–G; Supplementary Fig. S4B and S4C). However, AZD2811 nanoparticle at 98.7 mg/kg (the dose for which we observed the biggest impact on the bone marrow) induces a 55% and 60% reduction in the neutrophil count, respectively, at days 5 and 9, with recovery at day 15 (Fig. 4G; Supplementary Fig. S4C). The overall WBC count was not affected (Fig. 4F; Supplementary Fig. S4B). In addition to supporting the conclusion that AZD2811 nanoparticle impacts bone marrow at higher doses, this also suggests that peripheral neutrophil count could be used as a surrogate measure of the effect on bone marrow.

A high dose of AZD2811 nanoparticle extends overall survival in an AML disseminated xenograft model

Having established efficacy in subcutaneous xenograft models, we explored a high dose of AZD2811 nanoparticle in the disseminated xenograft model MOLM-13 in NOG mice. In this model, AML cells are introduced intravenously and proliferate in the blood. AZD2811 nanoparticle improved the median overall survival from 10 days in mice dosed with vehicle compared with 23.5 days with AZD2811 nanoparticle ($P < 0.0001$; Fig. 5A). In a separate experiment, mice given either one dose of vehicle or 98.7 mg/kg of AZD2811 nanoparticle were terminally sampled for peripheral blood and bone marrow at day 7 and 10 and day 7 and 14, respectively. Human CD45 and human HLA-ABC presence in peripheral blood or bone marrow was used to determine tumor load as the percentage of human cells in the sample. AZD2811 nanoparticle ablated the presence of tumor cells in the peripheral blood for at least 14 days (Fig. 5B) and in the bone marrow for at least 7 days (Fig. 5C). Even at day 14 following AZD2811 nanoparticle administration, the amount of tumor cells was less than 3% of the total bone marrow cells (Fig. 5C). In these mice,

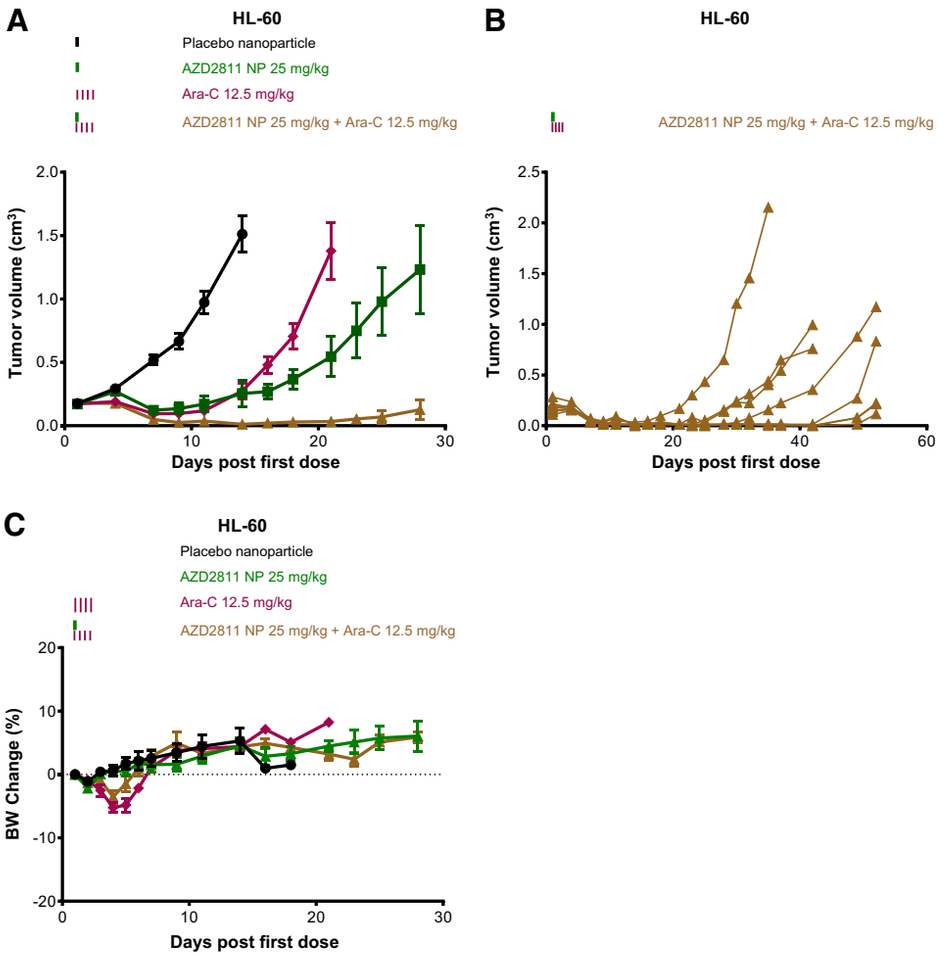

Figure 3.
The combination of AZD2811 nanoparticle and Ara-C prolonged the durability of response in the HL-60 AML xenograft model growth *in vivo*. **A,** TGI after one cycle of the AZD2811 nanoparticle or Ara-C monotherapy treatment or the combination of AZD2811 nanoparticle and Ara-C in the subcutaneous HL-60 xenograft model in CB17 SCID mice. Data are represented as mean ± SEM ($n = 10$ for placebo nanoparticle and $n = 8$ for AZD2811 nanoparticle-treated groups. **B,** TGI from individual mice ($n = 8$) after combining AZD2811 nanoparticle at 25 mg/kg administered on day 1 and day 3 with Ara-C at 12.5 mg/kg administered once daily for 4 consecutive days in CB17 SCID mice. **C,** Minimal body weight loss is observed with these efficacious doses use as monotherapy or in combination. Data expressed as percentage change in CB17 SCID mouse body weight relative to start body weight on day 0. Placebo nanoparticle, black circle; AZD2811 NP 25 mg/kg, green square; Ara-C 12.5 mg/kg, red diamond; AZD2811 NP 25 mg/kg + Ara-C 12.5 mg/kg, brown triangle.

AZD2811 nanoparticle was well tolerated at 98.7 mg/kg; no body weight loss was initially observed compared with predose start body weight, whereas the control group lost weight due to the rapid increase in tumor burden (Fig. 5D).

Multiple cycles of a high dose of AZD2811 nanoparticle causes profound regression and provides durability of response

To explore durability of response in more detail, two subcutaneous AML xenograft models, OCI-AML3 and MV-4-11, were dosed at 98.7 mg/kg weekly until complete regression was established. Therapy was then stopped and the regrowth of the tumors monitored. AZD2811 nanoparticle treatment results in sustained durability of response for 64 and 56 days, respectively (conclusion of study; Fig. 6A and B). AZD2811 nanoparticle was again well tolerated; minimal body weight loss was observed compared with predose start body weight (Fig. 6C and D). Collectively, these data establish that repeated cycles of AZD2811 nanoparticle can improve the duration of response in murine tumor models.

Discussion

AML remains a disease of high unmet need as few therapies are able to deliver durable benefit (3, 4). Barasertib (AZD1152), an intravenous prodrug rapidly converted to AZD2811, delivered promising clinical activity in elderly AML patients when delivered as a 7-day infusion (18). The preclinical data presented here supports the potential for the AZD2811 nanoparticle formulation to improve on the observations made with AZD1152. Preclinically, administration of the AZD2811 nanoparticle was efficacious across a range of AML xenograft models (HL-60, MV-4-11, and OCI-AML3), as well as the disseminated model MOLM-13.

The effects observed in the preclinical xenograft models suggest that AZD2811 delivered as a nanoparticle is able to achieve durable effects even in rapidly growing models. However, the limitation of the subcutaneous xenografts is that they grow as a solid mass, while patients have disease disseminated in the blood and bone marrow. Although this is challenging to model it was addressed by assessing the MOLM-13 disseminated tumor burden in the peripheral blood and in the bone marrow in mouse, and separately by exploring the effects of high-dose AZD2811 nanoparticle on bone marrow in rats and as a consequence on the complete blood count. In a disseminated model, AZD2811 nanoparticle sustains sufficient compound levels in both blood and bone marrow to reduce MOLM-13 cells and deliver increased animal survival. This suggests that the release rate does not limit the effectiveness of AZD2811 in the blood and the bone marrow, at least when administered at high doses.

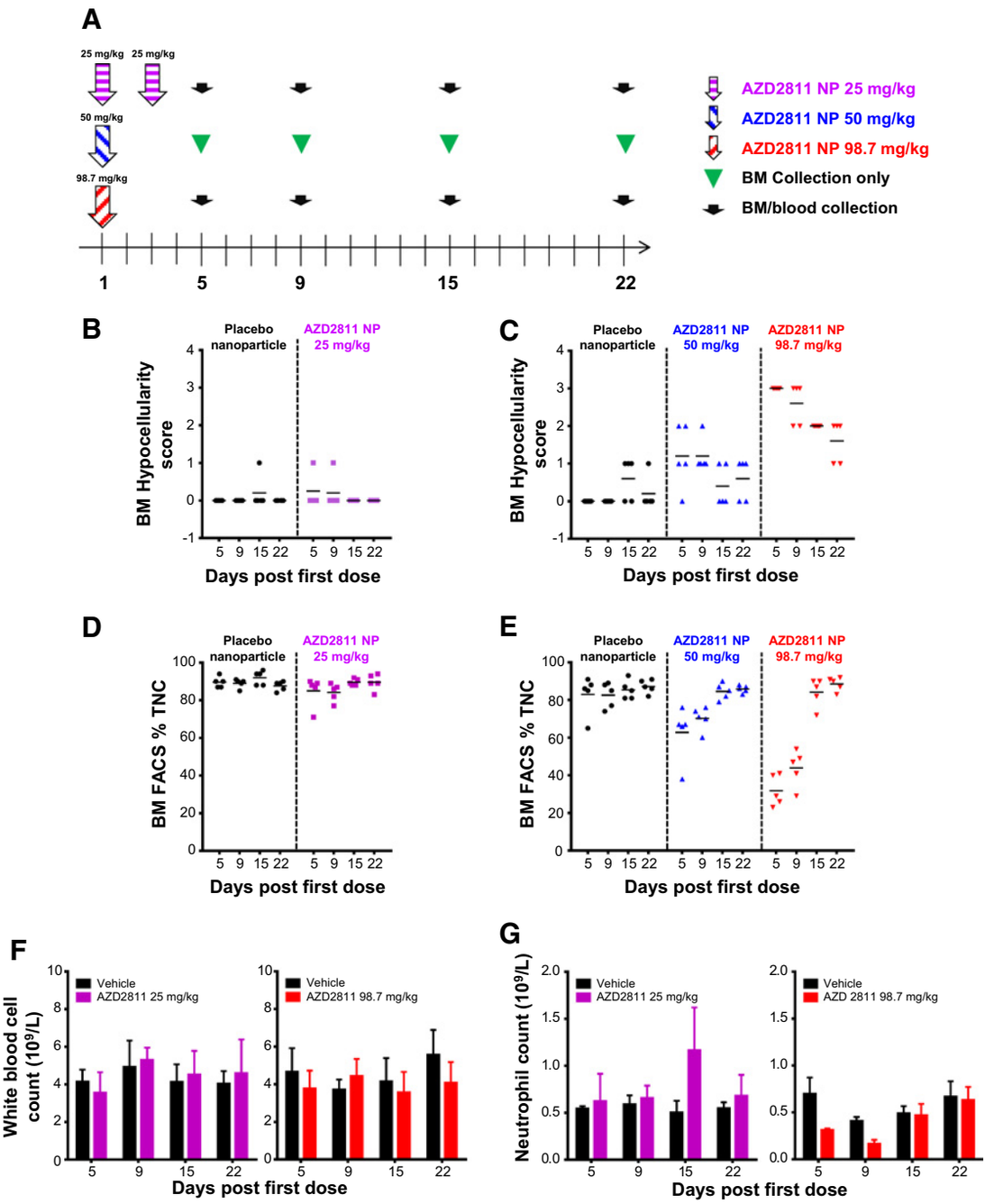

Figure 4.

AZD2811 nanoparticle affects the bone marrow cellularity and peripheral blood neutrophil count in a dose-dependent manner. **A,** Design of the preclinical study to evaluate the impact of AZD2811 nanoparticle treatment on the rat bone marrow (BM) and blood cellularity. **B** and **C,** Scatter dot plot of semiquantitative BM hypocellularity scores from H&E-stained sections of femur collected at 5, 9, 15, and 22 days following the first dose of AZD2811 nanoparticle. **D** and **E,** FACS analysis of percentage TNC from individual animal bone marrow aspirates taken at 5, 9, 15, and 22 days following the first dose of AZD2811 nanoparticle. WBC (**F**) and neutrophil (**G**) counts from peripheral blood samples taken at 5, 9, 15, and 22 days following the first dose of AZD2811 nanoparticle. Data are represented as mean ± SEM (n = 4–5).

The release characteristics of nanoparticle formulation of AZD2811 were selected to spare the bone marrow at efficacious doses to enable long-term dosing of the molecule, for solid tumors (19). Given that AML blasts initiate in the bone marrow, successful therapy needs to effectively treat disease in the bone marrow compartment, or patients are likely to relapse quickly. We

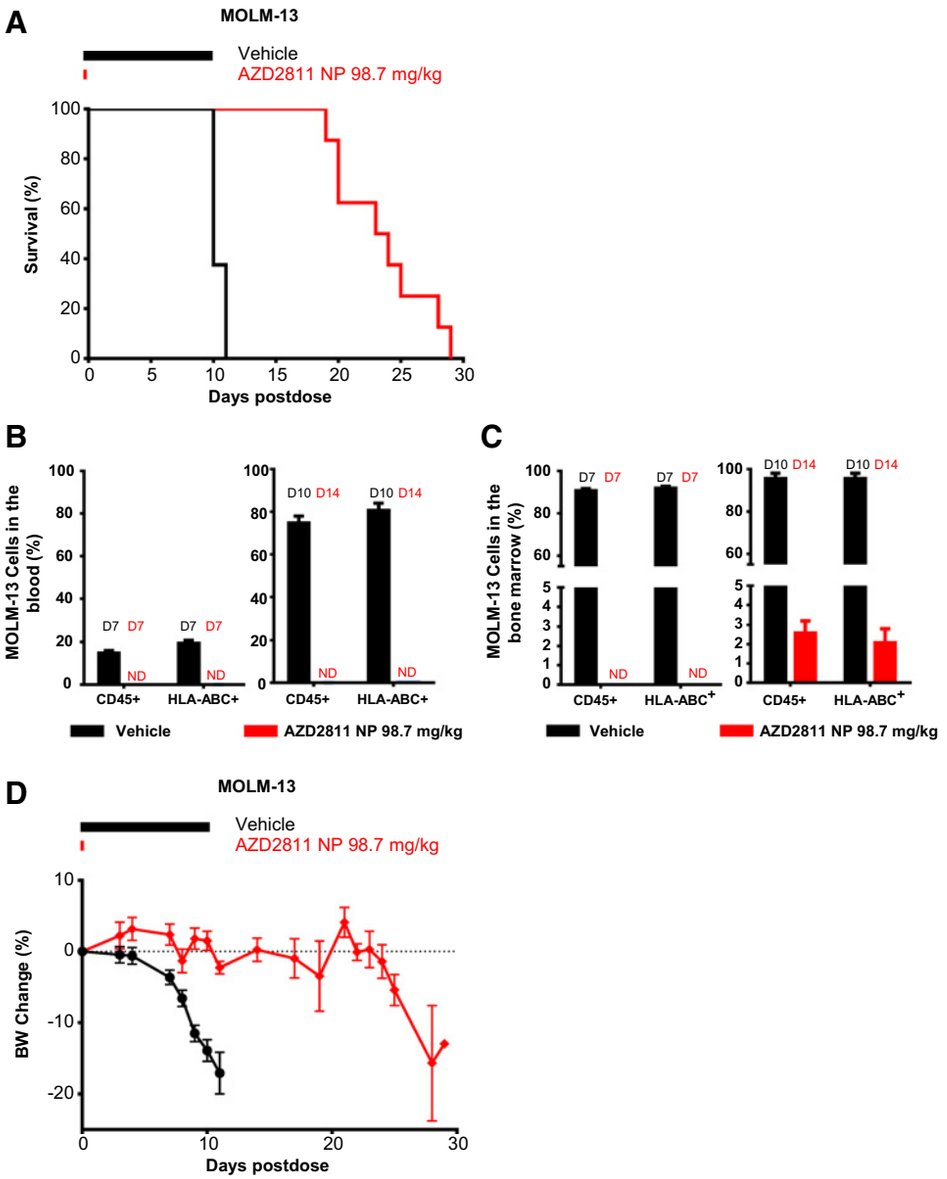

Figure 5.
AZD2811 nanoparticle prolongs the survival of NOG mice tail vein injected with MOLM-13 cells. **A**, Survival of NOG mice, tail vein injected in the disseminated MOLM-13 xenograft model, after one cycle of a high dose of AZD2811 nanoparticle ($n = 8$ per group treatment). Tumor load in (**B**) the peripheral blood and (**C**) the bone marrow 7 and 11 days after vehicle treatment or 7 and 14 days after a high dose of AZD2811 nanoparticle. **D**, Percentage changes in body weight relative to start body weight on day 0 of NOG mice bearing disseminated MOLM-13 xenograft model. Data are represented as mean ± SEM ($n = 8$ per group treatment). Vehicle, black circle; AZD2811 NP 98.7 mg/kg, red diamond. ND, nondetectable.

further explored the impact of dose on rat bone marrow cells. Reduction of cells in the bone marrow demonstrated the presence of sufficient concentration of AZD2811 in that compartment. At lower doses, the AZD2811 nanoparticle had minimal impact on the bone marrow consistent with previous observations (19). However, when administered at higher doses effects on bone marrow cellularity were clearly seen. The monotherapy induction of bone marrow hypocellularity in the rat supports the conclusion that following nanoparticle administration AZD2811 can distribute in sufficient concentrations to be active in the bone marrow. Therefore, adapting the dose of the AZD2811 nanoparticle should be able to achieve an efficient reduction of the blast number present in the bone marrow. A consequence of the effects of AZD2811 in the bone marrow is the reduction in peripheral blood neutrophil counts, providing an indirect approach to monitor the exposure and effects of AZD2811 in that compartment. The scope of this study did not allow for detailed exploration of relative sensitivity profiles for bone marrow and AML cells. However, given that we have clearly established that the AZD2811 nanoparticle administered at an appropriate dose has relevant exposure at the bone marrow, this provides a strong rationale that sufficient drug will access this compartment to treat bone marrow resident disease. To build on this, it would be informative to have greater insight into the relative sensitivity of AML cells versus normal cells. In particular, it will be important to consider both the time and concentration of exposure of bone marrow cells and AML tumor cells to AZD2811. Finally, there are currently no patient selection biomarkers that identify cells likely to exhibit increased sensitivity to treatment. This may help drive further rationalization of the treatment strategy in the clinic.

To explore the preclinical efficacy dose response to the AZD2811 nanoparticle, the HL-60 tumor xenograft was chosen as historically it was poorly sensitive to AZD1152, and therefore offered the ability to generate discriminating data. AZD2811

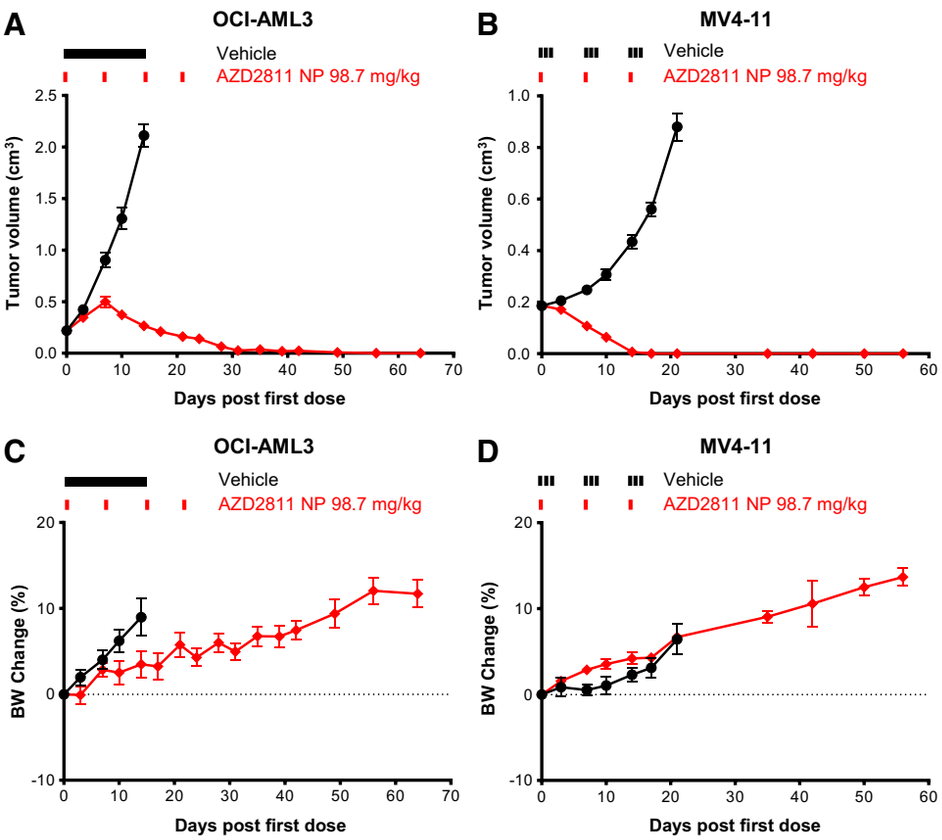

Figure 6.
AZD2811 nanoparticle given as monotherapy induces prolonged regression of the growth of AML xenograft models *in vivo*. **A**, Tumor growth inhibition after four cycles of the AZD2811 nanoparticle in the subcutaneous OCI-AML3 xenograft model in CB17 SCID mice. Data are represented as mean ± SEM ($n = 8$ per groups). **B,** Tumor growth inhibition after three cycles of the AZD2811 nanoparticle in the subcutaneous MV4-11 xenograft model in CB17 SCID mice. Data are represented as mean ± SEM ($n = 8$ per groups). **C** and **D,** No significant body weight loss is observed with these efficacious doses. Data expressed as percentage change in CB17 SCID mouse body weight relative to start body weight on day 0. Vehicle, black circle; AZD2811 NP 98.7 mg/kg, red diamond.

nanoparticle treatment of HL-60 tumor xenografts resulted in a reduction of tumor growth or regression across a range of doses. Notably, a single high dose of the AZD2811 nanoparticle delivered a durable response with tumors "cured" in a number of animals. Importantly, efficacy can be delivered flexibly, which gives the opportunity to modify both monotherapy and combination approaches. This flexibility can allow therapy to be tailored at the individual patient level. A common concern with cell-cycle inhibitors is the impact on the bone marrow or the gastrointestinal tract. Although this is less important when patients receive treatment for short periods of time, it is likely to be very important when maintaining patients whose disease is sensitive to AZD2811. This durability of response provided by the AZD2811 nanoparticle was further demonstrated in other AML preclinical models when dosed weekly at 98.7 mg/kg, mirroring the doses at which bone marrow reduction was observed.

Although the AZD2811 nanoparticle has sustained antitumor activity as a monotherapy, durability of response can also be achieved by combining a lower dose of the AZD2811 nanoparticle with Ara-C. A lower dose of the AZD2811 nanoparticle combined with Ara-C achieved greater durability of response than when either was used as monotherapy. Importantly, the dose response we have established shows that the AZD2811 nanoparticle can be combined with Ara-C at an exposure that does not impact peripheral blood neutrophils or bone marrow. This further highlights the flexibility of the nanoparticle formulation, and may provide durability of response potentially without exacerbating side effects when combining chemotherapy with cell-cycle inhibitors.

In a phase II study, for previously treated AML, barasertib given as a 7-day infusion improved the objective complete response rate by 35% versus 12% for LDAC (18). This study suggests that effective inhibition or arrest of the cell cycle has significant benefits for AML patients. Being able to increase the durability of inhibition and improve the way the drug is administered by using an approach such as the AZD2811 nanoparticle will contribute significantly to increasing the potential therapeutic benefit. The preclinical data presented here establishes that the AZD2811 nanoparticle has potential to improve on barasertib (AZD1152).

Disclosure of Potential Conflicts of Interest

M. Hattersley is an associate principal scientist and has ownership interest (including patents) in AstraZeneca. No potential conflicts of interest were disclosed by the other authors. All authors are current or former AstraZeneca employees and share holders.

Authors' Contributions

Conception and design: N. Floc'h, S. Ashton, E.J. Pease, S.T. Barry
Development of methodology: S. Wen
Acquisition of data (provided animals, acquired and managed patients, provided facilities, etc.): P. Taylor, E. Harris, R. Odedra, J. Caddy, M. Hattersley, S. Wen, J.E. Pilling
Analysis and interpretation of data (e.g., statistical analysis, biostatistics, computational analysis): N. Floc'h, S. Ashton, R. Odedra, K. Maratea, N. Derbyshire, V.N. Jacobs, M. Hattersley, N.J. Curtis, J.E. Pilling, S.T. Barry
Writing, review, and/or revision of the manuscript: N. Floc'h, S. Ashton, P. Taylor, K. Maratea, N. Derbyshire, M. Hattersley, N.J. Curtis, J.E. Pilling, E.J. Pease, S.T. Barry

Administrative, technical, or material support (i.e., reporting or organizing data, constructing databases): N. Floc'h, P. Taylor, D. Trueman, E. Harris, M. Hattersley, S. Wen, N.J. Curtis
Study supervision: N. Floc'h, S. Ashton, P. Taylor, M. Hattersley, S.T. Barry
Other (conception and design of studies): S. Ashton

Acknowledgments

We thank M. Dymond and M.A. Pilling for statistical support, staff in Laboratory Animal Sciences in Alderley Park and Gatehouse Park for technical support, BIND Therapeutics Inc., for providing the nanoparticle formulations, and Oncotest for delivering the MOLM-13 data.

The costs of publication of this article were defrayed in part by the payment of page charges. This article must therefore be hereby marked *advertisement* in accordance with 18 U.S.C. Section 1734 solely to indicate this fact.

Received September 9, 2016; revised October 11, 2016; accepted March 8, 2017; published OnlineFirst March 14, 2017.

References

1. Surveillance Epidemiology and End Results. SEER Stat Fact Sheets: acute myeloid leukemia (AML); 2015. Available from: http://seer.cancer.gov/statfacts/html/amyl.html.
2. The Cancer Genome Atlas Research Network. Genomic and epigenomic landscapes of adult de novo acute myeloid leukemia. N Engl J Med 2013;368:2059–74.
3. Dohner H, Estey EH, Amadori S, Appelbaum FR, Buchner T, Burnett AK, et al. Diagnosis and management of acute myeloid leukemia in adults: recommendations from an international expert panel, on behalf of the European LeukemiaNet. Blood 2010;115:453–74.
4. Coombs CC, Tallman MS, Levine RL. Molecular therapy for acute myeloid leukaemia. Nat Rev Clin Oncol 2016;13:305–18.
5. Dombret H, Gardin C. An update of current treatments for adult acute myeloid leukemia. Blood 2016;127:53–61.
6. Dohner H, Weisdorf DJ, Bloomfield CD. Acute myeloid leukemia. N Engl J Med 2015;373:1136–52.
7. Pettit K, Odenike O. Defining and treating older adults with acute myeloid leukemia who are ineligible for intensive therapies. Front Oncol 2015;5:280.
8. Oran B, Weisdorf DJ. Survival for older patients with acute myeloid leukemia: a population-based study. Haematologica 2012;97:1916–24.
9. Erba HP. Finding the optimal combination therapy for the treatment of newly diagnosed AML in older patients unfit for intensive therapy. Leuk Res 2015;39:183–91.
10. Hills RK, Burnett AK. Applicability of a "Pick a Winner" trial design to acute myeloid leukemia. Blood 2011;118:2389–94.
11. Fenaux P, Mufti GJ, Hellstrom-Lindberg E, Santini V, Gattermann N, Germing U, et al. Azacitidine prolongs overall survival compared with conventional care regimens in elderly patients with low bone marrow blast count acute myeloid leukemia. J Clin Oncol 2010;28:562–9.
12. Kantarjian HM, Thomas XG, Dmoszynska A, Wierzbowska A, Mazur G, Mayer J, et al. Multicenter, randomized, open-label, phase III trial of decitabine versus patient choice, with physician advice, of either supportive care or low-dose cytarabine for the treatment of older patients with newly diagnosed acute myeloid leukemia. J Clin Oncol 2012;30:2670–7.
13. Mortlock AA, Foote KM, Heron NM, Jung FH, Pasquet G, Lohmann JJ, et al. Discovery, synthesis, and *in vivo* activity of a new class of pyrazoloquinazolines as selective inhibitors of aurora B kinase. J Med Chem 2007;50:2213–24.
14. Yang J, Ikezoe T, Nishioka C, Tasaka T, Taniguchi A, Kuwayama Y, et al. AZD1152, a novel and selective aurora B kinase inhibitor, induces growth arrest, apoptosis, and sensitization for tubulin depolymerizing agent or topoisomerase II inhibitor in human acute leukemia cells *in vitro* and *in vivo*. Blood 2007;110:2034–40.
15. Wilkinson RW, Odedra R, Heaton SP, Wedge SR, Keen NJ, Crafter C, et al. AZD1152, a selective inhibitor of Aurora B kinase, inhibits human tumor xenograft growth by inducing apoptosis. Clin Cancer Res 2007;13:3682–8.
16. Boss DS, Witteveen PO, van der Sar J, Lolkema MP, Voest EE, Stockman PK, et al. Clinical evaluation of AZD1152, an i.v. inhibitor of Aurora B kinase, in patients with solid malignant tumors. Ann Oncol 2011;22:431–7.
17. Lens SM, Voest EE, Medema RH. Shared and separate functions of polo-like kinases and aurora kinases in cancer. Nat Rev Cancer 2010;10:825–41.
18. Kantarjian HM, Martinelli G, Jabbour EJ, Quintas-Cardama A, Ando K, Bay JO, et al. Stage I of a phase 2 study assessing the efficacy, safety, and tolerability of barasertib (AZD1152) versus low-dose cytosine arabinoside in elderly patients with acute myeloid leukemia. Cancer 2013;119:2611–9.
19. Ashton S, Song YH, Nolan J, Cadogan E, Murray J, Odedra R, et al. Aurora kinase inhibitor nanoparticles target tumors with favorable therapeutic index *in vivo*. Sci Transl Med 2016;8:325ra17.
20. Song YH, Shin E, Wang H, Nolan J, Low S, Parsons D, et al. A novel in situ hydrophobic ion paring (HIP) formulation strategy for clinical product selection of a nanoparticle drug delivery system. J Control Release 2016;229:106–19.
21. Kilkenny C, Browne WJ, Cuthill IC, Emerson M, Altman DG. Improving bioscience research reporting: the ARRIVE guidelines for reporting animal research. PLoS Biol 2010;8:e1000412.
22. Saad A, Palm M, Widell S, Reiland S. Differential analysis of rat bone marrow by flow cytometry. Comp Haematol Int 2001;10:97–101.
23. Oke A, Pearce D, Wilkinson RW, Crafter C, Odedra R, Cavenagh J, et al. AZD1152 rapidly and negatively affects the growth and survival of human acute myeloid leukemia cells *in vitro* and *in vivo*. Cancer Res 2009;69:4150–8.
24. Friberg LE, Sandstrom M, Karlsson MO. Scaling the time-course of myelosuppression from rats to patients with a semi-physiological model. Invest New Drugs 2010;28:744–53.